



THE UNIVERSITY *of* EDINBURGH

Edinburgh Research Explorer

Realization of a graphene/PMMA acoustic capacitive sensor released by silicon dioxide sacrificial layer

Citation for published version:

Xu, J, Wood, G, Mastropaolo, E, Newton, MJ & Cheung, R 2021, 'Realization of a graphene/PMMA acoustic capacitive sensor released by silicon dioxide sacrificial layer', *ACS Applied Materials & Interfaces*, pp. 1-11. <https://doi.org/10.1021/acscami.1c05424>

Digital Object Identifier (DOI):

[10.1021/acscami.1c05424](https://doi.org/10.1021/acscami.1c05424)

Link:

[Link to publication record in Edinburgh Research Explorer](#)

Document Version:

Publisher's PDF, also known as Version of record

Published In:

ACS Applied Materials & Interfaces

General rights

Copyright for the publications made accessible via the Edinburgh Research Explorer is retained by the author(s) and / or other copyright owners and it is a condition of accessing these publications that users recognise and abide by the legal requirements associated with these rights.

Take down policy

The University of Edinburgh has made every reasonable effort to ensure that Edinburgh Research Explorer content complies with UK legislation. If you believe that the public display of this file breaches copyright please contact openaccess@ed.ac.uk providing details, and we will remove access to the work immediately and investigate your claim.



Realization of a Graphene/PMMA Acoustic Capacitive Sensor Released by Silicon Dioxide Sacrificial Layer

Jing Xu,* Graham. S. Wood, Enrico Mastropaolo, Michael. J. Newton, and Rebecca Cheung*

Cite This: <https://doi.org/10.1021/acsami.1c05424>

Read Online

ACCESS |

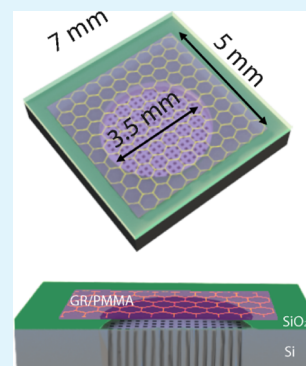
Metrics & More

Article Recommendations

Supporting Information

ABSTRACT: We report the realization of an acoustic capacitive microphone formed by graphene/poly(methyl methacrylate) (PMMA). It is the first time that the ultra-large graphene/PMMA membrane suspended fully over the cavity has been fabricated by releasing the silicon dioxide sacrificial layer underneath the membrane. The novelty in the fabrication method is that the silicon dioxide layer has been etched by hydrogen fluoride vapor from the back of the partly etched silicon substrate. Using the new process, the ultra-large graphene/PMMA membrane, with a diameter to thickness ratio of 7800, has been suspended over the cavity with a 2 μm air gap. The spacing of 2 μm is the minimum gap over the graphene-based acoustic capacitive microphones which have been reported so far. The static deformation of the suspended graphene/PMMA membrane after silicon dioxide has been etched is estimated to be 270 nm. The aspect ratio of the membrane's diameter over its static deformation is around 13,000, which shows that the graphene/PMMA membrane with a diameter of a few millimeters can be transferred and suspended over the substrate with relatively small deformation by releasing the sacrificial silicon dioxide layer. The dynamic behavior of the device under electrostatic actuation has been characterized. The acoustic response of the graphene/PMMA capacitive microphone has been measured, and the sensitivity has been observed to be $-47.5 \text{ dB V (4.22 mV/Pa)} \pm 10\%$. The strain in the graphene/PMMA membrane is estimated to be 0.034%.

KEYWORDS: graphene, graphene transfer, audio sensing, electrostatic, MEMS



INTRODUCTION

Graphene has many attractions for the research and industrial communities since it was discovered¹ due to its remarkable electrical and mechanical properties, including ultra-high Young's modulus ($\sim 0.5\text{--}1 \text{ TPa}$), mechanical strength ($\sim 130 \text{ GPa}$), high electron mobility ($200,000 \text{ cm}^2 \text{ V}^{-1} \text{ s}^{-1}$),² and super low mass density (2200 kg/m^3). The attractive properties of graphene show its potential applications in pressure sensors,³ electromechanical actuators,⁴ resonators,^{5–9} biosensors,¹⁰ and microdrums.¹¹

For acoustic sensors, graphene is also a desirable material. Compared to polysilicon or silicon nitride membranes used in the commercial microphones, graphene-based membranes possess the potential of achieving high-sensitivity microphones due to the small thickness and low mass density. However, for sensing audio frequency (20 Hz to 20 kHz), the diameter of the graphene-based membrane reported in graphene-based acoustic sensors has been required to be a few millimeters (3.5–7 mm).^{12–16} Considering that the multi-layer graphene membrane is about a few atoms thick, it is challenging to transfer graphene due to the large aspect ratio of the membrane. So far, there have been a few acoustic applications based on graphene.^{12–19} In recent research, the graphene membrane has been thickened by increasing the graphene layer number ranging from 67¹² to 1800¹⁴ or by attaching 200 nm¹⁵ or micrometer thick poly(methyl methacrylate) (PMMA)¹⁴ in

order to increase the stability of the devices. A 10-layer graphene diaphragm with up to a 4 mm diameter has been fabricated but with a complex vacuum-assisted sublimation transfer method.¹⁶ Additionally, unlike the precise process of fabricating the commercial capacitive microphones where the diaphragm and backplate electrode have been fabricated onto one substrate,²⁰ the graphene-based acoustic sensor has been processed with a two-step method: the flexible graphene-based membrane has been transferred first onto a ring or a spacer to serve as a diaphragm with the support; then, the supported membrane has been assembled manually into the case or cartridge^{12–16} with the backplate electrode inside to form the capacitive microphone. The two-step fabrication method increases the complexity and decreases the consistency of the sensors, which limits its application in the further minimization of the air gap. The air gap of the sensors with a diameter of a few millimeters in the literature has been reported to be from 8.8 to 172 μm .^{12–16} The air gap of the devices is a variable parameter which could not be controlled due to the manual

Received: March 23, 2021

Accepted: June 27, 2021

Table 1. Comparison of Our Work to Other Research on Graphene-Based Acoustic Sensors

membrane type	references	air gap	fabrication	bias voltage (V)	sensitivity (dB V)
300-layer graphene	13	18.6 μm	dry transfer with the PET support ring	200	-60
1800-layer graphene and 2 μm PMMA	14	10 μm	dry transfer with the gold support ring	N/A	-20
Monolayer graphene and 200 nm PMMA	our work ¹⁵	8.8 μm	dry transfer with the silicon support ring	1	-60
10-layer graphene	16	172 μm	vacuum-assisted sublimation transfer on the partly open substrate	200	-60
6-layer graphene and 450 nm PMMA	this work	2 μm	silicon dioxide as the sacrificial layer	2.6	-47.5

assembly. Furthermore, the bias voltages of the graphene-based acoustic sensors with more than 100 μm have been reported to be 50 and 200 V DC^{12,16} to boost the sensitivity of acoustic response, which limits the potential of integrating the graphene-based devices on the smart phone, hearing aid, or other wearable electronic devices. To improve the acoustic sensors' sensitivity, it is critical to minimize the air gap distance between the membrane and the substrate, thus maximizing the variable capacitance generated by sound pressure and accordingly the capacitance of the static graphene-based microphone. Therefore, the development of a new process for minimizing the air gap between the membrane and the substrate is essential in improving the performance of the graphene-based acoustic sensors.

Releasing graphene by etching the silicon dioxide underneath with hydrogen fluoride (HF) acid has been reported to form cantilever²¹ or bridge²²⁻²⁴ devices in graphene nanomechanical systems. The length of the graphene membrane in the nanomechanical devices has been shown to be a few micrometers, and the thickness of silicon dioxide has been designed to be around 300 nm.²¹⁻²⁴ Using HF acid to etch the silicon dioxide sacrificial layer for the development of the micrometer-size graphene-based fully clamped microphone could be difficult. The diameter of the graphene-based membrane over the thickness of the silicon dioxide layer should be designed to be around 1000 to achieve the relatively large capacitance and improved performance of the graphene-based microphone, which can increase the complexity of releasing the graphene-based membrane by etching silicon dioxide. Additionally, unlike the cantilever and bridge structure, the etchant could flow from the sides of graphene to etch the oxide. The fully clamped design increases the difficulty to etch silicon dioxide.

We have developed a process involving the etching of a silicon dioxide sacrificial layer to form an ultra-large graphene/PMMA membrane microphone. The sacrificial layer can be used to control the distance of the air gap between the membrane and the substrate with the electrode. It is the first time ultra-large graphene/PMMA has been suspended fully over a closed cavity by sacrificing a silicon dioxide layer. The thickness of the silicon dioxide layer can be changed with a view to optimize the capacitance of the device and the total acoustic/mechanical (i.e., vibroacoustic) damping. The diameter to thickness ratio of the sacrificial silicon dioxide in our work is about 1750. The difficulties in the method are to etch the thin silicon dioxide layer under the fully clamped large area of the graphene/PMMA membrane and to prevent the membrane from being attached to the substrate. Henceforth, around 1500 square holes with a 50 μm diameter have been designed and etched into the silicon substrate from the back. Then, the sacrificial layer is etched from the back side of the substrate by HF vapor in the oxide etcher (Xeric Oxide Etch,

memsstar). HF vapor has been used instead of HF liquid in order to decrease the humidity and to prevent stiction between the membrane and substrate.

In this work, with the new transfer method, an air gap of 2 μm has been achieved, which is the minimum spacing that has been reported, as shown in Table 1, giving a capacitance of 26.3 pF estimated from eq 1

$$C = \frac{\epsilon A}{d} \quad (1)$$

where C is the capacitance of the device, ϵ refers to the permittivity of dielectric, A is the area of plate overlap in square meters, and d is the distance between plates in meters.

The device has been actuated electrostatically, and the resonant frequency under electrostatic actuation has been measured to be around 8.96 kHz \pm 2%, which is within the audio frequency range (20 Hz to 20 kHz). In the case of the acoustic actuation, the device has been connected to the gate of a MOSFET with a relatively small bias voltage of 2.6 V DC. The acoustic sensitivity of the sample has been measured to be around -47.5 dB V. The sensitivity of the graphene-based microphone has been reported to be from -60 to -20 dB V.¹³⁻¹⁶ The sensitivity of the device reported here is comparable with those reported in other works.

EXPERIMENTAL SECTION

Operating Principles and Methods. Figure 1a shows the optical microscopy image of the graphene/PMMA electrostatic microphone. The graphene-based membrane consists of 450 nm PMMA and 6-layer graphene. The silver paste has been used to make contact to the graphene/PMMA membrane for electrostatic actuation. The membrane has been suspended over a 3.5 mm diameter cavity. As shown in Figure 1b, the graphene/PMMA membrane has been clamped fully over the silicon dioxide anchor on the silicon substrate. The air gap between the membrane and the substrate has been measured to be around 2 μm under a Leica 150x optical microscope. The graphene/PMMA membrane and the silicon substrate work as two plates for the capacitive structure. The natural frequency formula for the graphene/PMMA membrane can be expressed as

$$t_{\text{eff}} = t_g + t_p \quad (2)$$

$$\rho_{\text{eff}} = \frac{\rho_g t_g + \rho_p t_p}{t_g + t_p} \quad (3)$$

$$A_m = \frac{2\rho_{\text{air}} R}{3\rho_{\text{eff}} t_{\text{eff}}} \quad (4)$$

$$f_{\text{mn}} = \frac{\beta_{\text{mn}}}{2\pi R} \sqrt{\frac{N_i + N_a}{\rho_{\text{eff}} t_{\text{eff}} (1 + A_m)}} \quad (5)$$

where t and ρ are the thickness and density of the material, respectively; t_{eff} and ρ_{eff} refer to the effective thickness and effective density for the graphene (g)/PMMA (p) bilayer membrane,

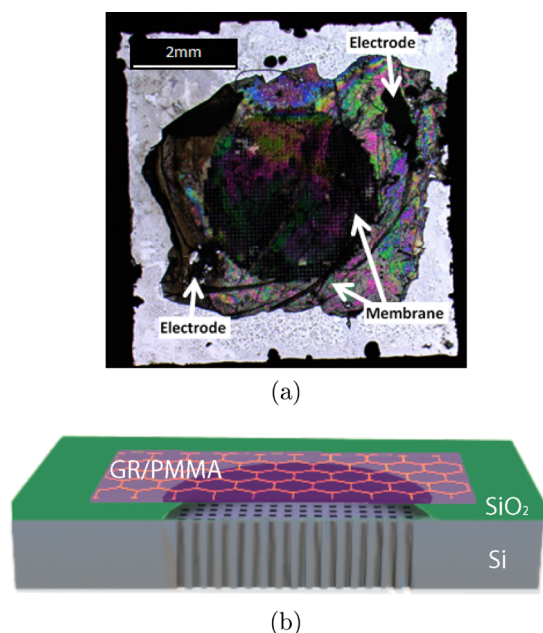


Figure 1. Optical microscopy image (a) and cross-section schematic (b) of the graphene-based electrostatic microphone.

respectively; R is the radius of the membrane; ρ_{air} is the air density; A_m is the air mass; N_i and N_a represent the built-in tension and the tension caused by the dynamic actuation, respectively; and β_{mn} is a dimensionless coefficient of the resonant mode.

Fabrication. The fabrication schematic is depicted in Figure 2a. First, $2.3 \mu\text{m}$ thick silicon dioxide has been deposited on the p-type silicon substrate in which the resistivity is $1\text{--}10 \Omega\text{cm}$. The silicon

substrate has been used as the bottom electrode in the electrostatic actuation configuration. After that, around 1500 square vent holes with a $50 \mu\text{m}$ width have been patterned within a 3.5 mm diameter circle and then etched into silicon from the back side of the substrate. The membrane consisting of 6-layer graphene and 450 nm PMMA has been dry-transferred on the silicon dioxide substrate, and the details of the dry-transfer method are shown in ref 19. Last, the graphene/PMMA membrane has been released with HF vapor flowing through the partly etched silicon substrate to remove silicon dioxide. In this way, the graphene-based membrane has been suspended over the silicon dioxide anchor, with an air gap of around $2 \mu\text{m}$. The cross-section of the sample in each fabrication process is illustrated in Figure 2bI–IV accordingly.

Figure 2c,d shows the optical microscopy image before and after the silicon dioxide sacrificial layer has been etched. The thickness of silicon dioxide changes the reflectivity of the visible light under the microscope. Therefore, the color of the graphene-based membrane appears to be changed when silicon dioxide has been etched. With silicon dioxide as the sacrificial layer, the ultra-large graphene-based membrane can be transferred over the air gap of $2 \mu\text{m}$. The use of HF vapor reduces the humidity of the membrane in order to avoid the membrane being stuck on the substrate. The vent holes are designed for allowing the HF vapor to flow in to perform the etch release and also for reducing the damping of a device with such a small air gap.

The PMMA-laminated layer has supported the graphene layer in the dry-transfer method and the process of silicon dioxide etch release. The interface of the graphene/PMMA membrane and silicon dioxide allows the millimeter-size membrane to be suspended fully over the closed cavity. The silicon dioxide on silicon has been designed to be the substrate for the graphene/PMMA membrane to be transferred onto. In addition, silicon dioxide has worked as a sacrificial layer to control the air gap between the membrane and substrate.

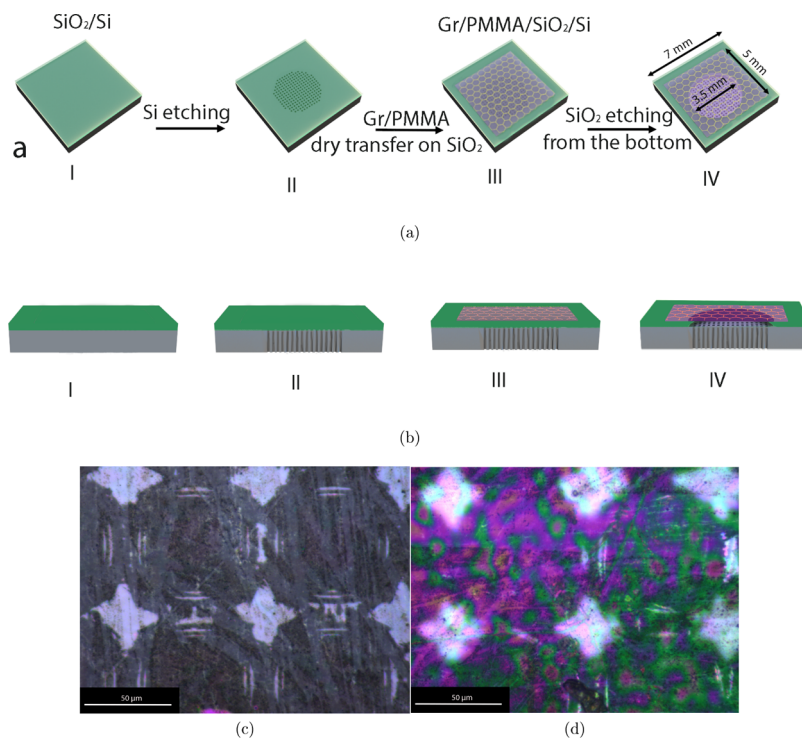


Figure 2. (a) (I) Deposition of $2.3 \mu\text{m}$ silicon dioxide on the p-type substrate; (II) patterning and etching of the $50 \mu\text{m}$ width vent holes into silicon from the back; (III) dry transfer of the graphene-based membrane on the silicon dioxide layer; (IV) etching of the silicon dioxide sacrificial layer via HF vapor (the diameters of the substrate, graphene/PMMA, and the partly open cavity have been designed to be around 7 mm , approximately 5 mm , and 3.5 mm , respectively); (b) cross-section of the graphene/PMMA microphone during the process; suspended graphene-based membrane before (c) and after (d) the sacrificial silicon dioxide etch.

RESULTS AND DISCUSSION

The graphene/PMMA closed cavity resonator has been characterized using a Polytec laser doppler vibrometer (LDV). The Raman spectra recorded by Raman Spectroscopy (inVia Renishaw) have been shown in the [Supporting Information](#). All measurements have been conducted on one device at room temperature and under atmospheric pressure.

Capacitance. As mentioned above, the capacitance between the membrane and the substrate is calculated to be 26.3 pF. Under the measurement of an HP 4280A 1 MHz CV meter, the capacitance is measured to be 26.2 pF. From the capacitance measurement, the air gap of the sample is estimated to be around 2.03 μm . Considering that the sacrificial silicon oxide layer is measured to be 2.3 μm thick, the average deformation of the membrane has been estimated to be about 270 nm when using this transfer method. The aspect ratio of the membrane's diameter over its static deformation is estimated to be around 4500. Therefore, the ultra-large graphene-based membrane has been transferred to the substrate with small static deformation.

Electrostatic Actuation. The graphene-based membrane has been actuated electrostatically by the bottom silicon substrate (in which the resistivity is 1–10 Ωcm) with the AC voltage ranging from 6 to 10 V and a constant 0.01 V DC voltage. The frequency response and mode shape of the membrane have been measured using LDV. As shown in [Figure 3a](#), the resonant frequency has been measured to be around 8.96 kHz \pm 2%. The quality factor of the device is estimated to be 1.53 \pm 5%. The wide shape of the frequency response might be due to the large damping generated by the small air gap. The velocity of the graphene/PMMA membrane at a resonant frequency of around 8.96 kHz has been observed to change from 5.79 to 17.56 $\mu\text{m/s}$ with increasing AC voltage. The sensitivity of the velocity is shown in [Figure 3b](#). The black squares represent the measured velocity of the membrane with a 6–10 V actuation AC voltage, while the red dashed line indicates the linear fitting. No resonance has been observed below 6 V AC, which might be due to the effect of damping and the relatively large resistance of the p-type silicon and the silver paste used to contact the sample. The sensitivity of the resonant vibration velocity has been estimated to be 2 $\mu\text{m/s}$ by the slope of the linear fitting. The mode shape, which is shown in [Figure 3c](#), illustrates that the membrane has been actuated under the (1, 1) mode at the resonant frequency of 8.96 kHz. The absence of the (0, 1) mode also suggests the presence of damping of the sample.

Strain Analysis. The total tension in the graphene/PMMA membrane under electrostatic actuation has been calculated with [eq 5](#), and the results are shown in [Table 2](#). In our other work,^{19,25} the bilayer membranes have been suspended over the same cavity diameter, but the graphene-transfer methods are different. In comparison to similar samples actuated electrothermally by 1 V AC and 1 V DC,^{19,25} the tension and strain in this work are the minimum.

The increasing DC voltage might increase the electrical stiffness and soften the strain in the membrane, and thus, the nonlinear response might be observed.²⁶ A DC voltage of 0.01 V has been applied to this work, which is supposed to minimize the electrical softening, compared to our work.^{19,25} In the suspended graphene/PMMA structure, the built-in tension dominates the overall tension.^{19,25} The decrease in the overall tension ($N_i + N_a$) in this work might indicate that using

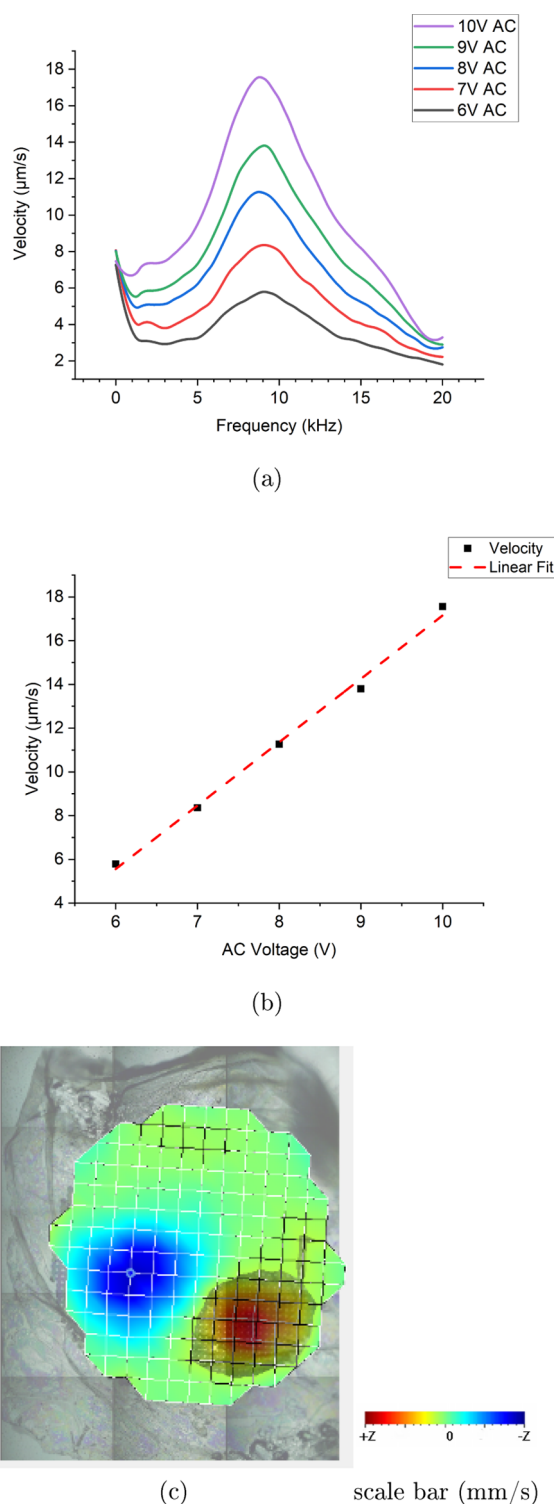


Figure 3. (a) Frequency response and (b) velocity sensitivity of the device by electrostatic actuation varying the AC voltage from 6 to 10 V; (c) mode shape for the 3.5 mm diameter graphene/PMMA membrane at a frequency of 9.10 kHz actuated by 9 V AC.

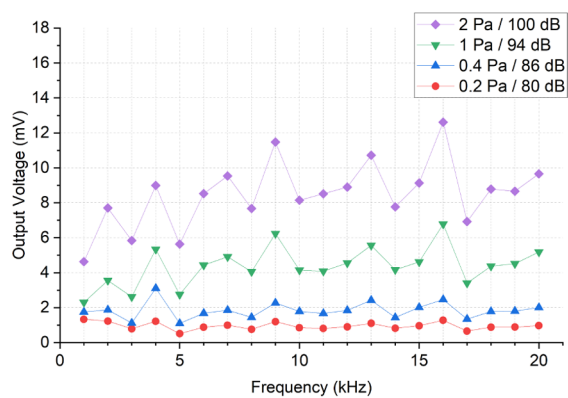
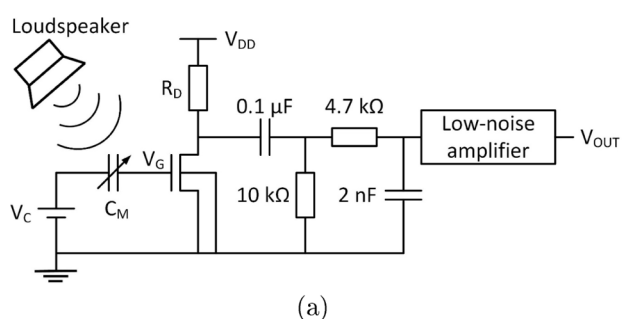
the silicon dioxide sacrificial layer compensates the built-in stress generated in the graphene-transfer method.

Acoustic Actuation. The graphene-based electrostatic microphone has been connected to an n-channel depletion mode MOSFET in order to measure the electronic signal transduced by the audio signal. The schematic measurement

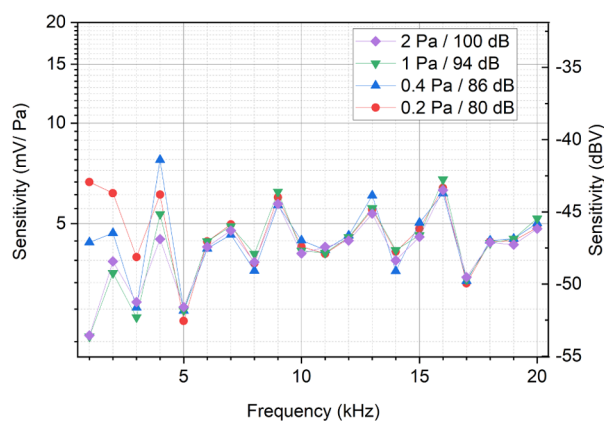
Table 2. Comparison of the Tension and Strain to Similar Designs

references	actuation method	actuation voltage	types of the devices' substrates	graphene-transfer method	tension (N/m)	strain (%)
our work ²⁵	electrothermal	1 V AC 1 V DC	open cavity	wet transfer	1.89	0.048
our work ¹⁹	electrothermal	1 V AC 1 V DC	closed cavity with a 220 μm spacing	dry transfer	1.53	0.041
this work	electrostatic	6 V AC 0.01 V DC	a 2.2 μm air gap with multiple vent holes	released by etching the sacrificial silicon dioxide layer	1.26	0.034

circuit setup is illustrated in Figure 4a. C_M represents the capacitance of the graphene-based microphone, which is variable when the sound pressure from the loudspeaker changes. The graphene-based microphone (C_M) applied with



(b)



(c)

Figure 4. (a) Schematic of the measurement circuit under acoustic actuation; the output voltage response (b) and the output voltage sensitivity (c) of the graphene-based electrostatic microphone system.

a bias voltage (V_C) of 2.6 V is connected to the gate of the MOSFET. The gate voltage (V_G) of the MOSFET has been measured to be 0.1 V, which suggests that the voltage drop across C_M is 2.5 V when the graphene-based electrostatic microphone is without acoustic actuation. The drain supply voltage (V_{DD}) and drain resistor (R_D) have been set to 13 V and 380 Ω , respectively. When the graphene-based membrane has been actuated by the sound pressure, V_G varies with change of the voltage drop across C_M . Therefore, the drain current (I_D) of the MOSFET changes. The drain has been connected to a band-pass filter in which the lower and upper cutoff frequencies are designed to be 159 Hz and 16.8 kHz, respectively. A low-noise audio amplifier (Zoom F4 Multi-Track Field Recorder) has been connected to the readout circuit output, giving the output voltage (V_{OUT}) with a voltage gain of 5. The graphene-based electrostatic microphone has been actuated by the sound pressure from 0.2 Pa (80 dB) to 2 Pa (100 dB). The measurement has been conducted from 1 to 20 kHz with a 1 kHz step. As shown in Figure 4b, V_{OUT} has been measured to vary from 0.5 to 13 mV with increasing sound pressure. The output voltage has been observed to ascend with the increasing sound pressure. The output voltage sensitivity has been estimated by the output voltage over the sound pressure. Dividing the sensitivity value relative to 1 V/Pa has been expressed in dB V, which is illustrated in Figure 4c. The sensitivity of the device has been estimated to be around -47.5 dB V (4.22 mV/Pa) \pm 10%. At frequencies between 1 and 4 kHz, a change in the sensitivity as a function of sound pressure is evident, as shown in Figure 4c. The observation could be related to the damping effect²⁷ and a smaller signal to noise ratio in the lower-frequency range. The device's sensitivity as a function of sound pressure is observed to be relatively constant with an average variation of 0.02 mV/Pa in the frequency range from 5 to 20 kHz.

CONCLUSIONS

The fabrication and characterization of a graphene/PMMA electrostatic microphone are reported. A novel process of using silicon dioxide as the sacrificial layer has been developed. It is the first time that an ultra-large graphene-based membrane has been suspended over the substrate with a 2 μm air gap and actuated electrostatically. Using the new processing method, an ultra-large graphene-based capacitor has been fabricated controllably to minimize the spacing between the membrane and substrate. From Raman spectra, the strain of the membrane has been estimated to be around 0.034%. The frequency response of the graphene/PMMA microphone under electrostatic actuation shows that the resonant frequency of the device is around 8.96 kHz \pm 2%. The velocity of the graphene/PMMA membrane under resonance has been observed to be linear with input AC voltage. The acoustic response with a sensitivity of -47.5 dB V (4.22 mV/Pa) \pm 10% has been estimated, which is comparable with that of

research in similar fields, suggesting the potential of commercial microphone development with good performance.

■ ASSOCIATED CONTENT

SI Supporting Information

The Supporting Information is available free of charge at <https://pubs.acs.org/doi/10.1021/acsami.1c05424>.

Raman spectrum of the graphene layer (PDF)

■ AUTHOR INFORMATION

Corresponding Authors

Jing Xu – *The School of Engineering, Institute for Integrated Micro and Nano Systems, University of Edinburgh, Edinburgh EH9 3FF, U.K.*; orcid.org/0000-0001-7122-4026; Email: jing.xu.2@ed.ac.uk

Rebecca Cheung – *The School of Engineering, Institute for Integrated Micro and Nano Systems, University of Edinburgh, Edinburgh EH9 3FF, U.K.*; Email: r.cheung@ed.ac.uk

Authors

Graham. S. Wood – *The School of Engineering, Institute for Integrated Micro and Nano Systems, University of Edinburgh, Edinburgh EH9 3FF, U.K.*; orcid.org/0000-0003-4973-813X

§Enrico Mastropaolo – *The School of Engineering, Institute for Integrated Micro and Nano Systems, University of Edinburgh, Edinburgh EH9 3FF, U.K.*

Michael. J. Newton – *The Acoustics and Audio Group, University of Edinburgh, Edinburgh EH8 9DF, U.K.*

Complete contact information is available at:

<https://pubs.acs.org/doi/10.1021/acsami.1c05424>

Notes

The authors declare no competing financial interest.

§Deceased 15th July 2019.

■ ACKNOWLEDGMENTS

The authors acknowledge the financial support of the UK Engineering and Physical Sciences Research Council (EPSRC). The authors genuinely acknowledge the assistance from Dr. Andrey Gromov for Raman spectroscopy measurements and Dr. Tony O'Hara (Memstar Ltd.) for developing the oxide etching process.

■ REFERENCES

- (1) Novoselov, K. S.; Geim, A. K.; Morozov, S. V.; Jiang, D.; Zhang, Y.; Dubonos, S. V.; Grigorieva, I. V.; Firsov, A. A. Electric Field Effect in Atomically Thin Carbon Films. *science* **2004**, *306*, 666–669.
- (2) Bolotin, K. I.; Sikes, K. J.; Jiang, Z.; Klima, M.; Fudenberg, G.; Hone, J.; Kim, P.; Stormer, H. L. Ultrahigh Electron Mobility in Suspended Graphene. *Solid State Commun.* **2008**, *146*, 351–355.
- (3) Aguilera-Servin, J.; Miao, T.; Bockrath, M. Nanoscale Pressure Sensors Realized from Suspended Graphene Membrane Devices. *Appl. Phys. Lett.* **2015**, *106*, 083103.
- (4) Zhu, S.-E.; Shabani, R.; Rho, J.; Kim, Y.; Hong, B. H.; Ahn, J.-H.; Cho, H. J. Graphene-based Bimorph Microactuators. *Nano Lett.* **2011**, *11*, 977–981.
- (5) Lee, S.; Chen, C.; Deshpande, V. V.; Lee, G.-H.; Lee, I.; Lekas, M.; Gondarenko, A.; Yu, Y.-J.; Shepard, K.; Kim, P.; Hone, J. Electrically Integrated SU-8 Clamped Graphene Drum Resonators for Strain Engineering. *Appl. Phys. Lett.* **2013**, *102*, 153101.
- (6) Wong, C.-L.; Annamalai, M.; Wang, Z.-Q.; Palaniapan, M. Characterization of Nanomechanical Graphene Drum Structures. *J. Micromech. Microeng.* **2010**, *20*, 115029.

(7) Weber, P.; Güttinger, J.; Tsioutsios, I.; Chang, D. E.; Bachtold, A. Coupling Graphene Mechanical Resonators to Superconducting Microwave Cavities. *Nano Lett.* **2014**, *14*, 2854–2860.

(8) Mathew, J. P.; Patel, R. N.; Borah, A.; Vijay, R.; Deshmukh, M. M. Dynamical Strong Coupling and Parametric Amplification of Mechanical Modes of Graphene Drums. *Nat. Nanotechnol.* **2016**, *11*, 747–751.

(9) Dolleman, R. J.; Davidovikj, D.; Cartamil-Bueno, S. J.; van der Zant, H. S. J.; Steeneken, P. G. Graphene Squeeze-film Pressure Sensors. *Nano Lett.* **2016**, *16*, 568–571.

(10) Pumera, M. Graphene in biosensing. *Mater. Today* **2011**, *14*, 308–315.

(11) Wang, Q.; Hong, W.; Dong, L. Graphene “Microdrums” on A Freestanding Perforated Thin Membrane for High Sensitivity MEMS Pressure Sensors. *Nanoscale* **2016**, *8*, 7663–7671.

(12) Zhou, Q.; Zheng, J.; Onishi, S.; Crommie, M. F.; Zettl, A. K. Graphene Electrostatic Microphone and Ultrasonic Radio. *Proc. Natl. Acad. Sci. U.S.A.* **2015**, *112*, 8942–8946.

(13) Todorović, D.; Matković, A.; Miličević, M.; Jovanović, D.; Gajić, R.; Salom, I.; Spasenović, M. Multilayer Graphene Condenser Microphone. *2D Materials* **2015**, *2*, 045013.

(14) Woo, S.; Han, J.-H.; Lee, J. H.; Cho, S.; Seong, K.-W.; Choi, M.; Cho, J.-H. Realization of a High Sensitivity Microphone for a Hearing Aid Using a Graphene-PMMA Laminated Diaphragm. *ACS Appl. Mater. Interfaces* **2017**, *9*, 1237–1246.

(15) Wood, G. S.; Torin, A.; Al-mashaal, A. K.; Smith, L. S.; Mastropaolo, E.; Newton, M. J.; Cheung, R. Design and Characterization of a Micro-Fabricated Graphene-Based MEMS Microphone. *IEEE Sens. J.* **2019**, *19*, 7234–7242.

(16) Carvalho, A. F.; Fernandes, A. J. S.; Ben Hassine, M.; Ferreira, P.; Fortunato, E.; Costa, F. M. Millimeter-sized Few-layer Suspended Graphene Membranes. *Appl. Mater. Today* **2020**, *21*, 100879.

(17) Zhou, Q.; Zettl, A. Electrostatic Graphene Loudspeaker. *Appl. Phys. Lett.* **2013**, *102*, 223109.

(18) Al-Mashaal, A. K.; Wood, G. S.; Torin, A.; Mastropaolo, E.; Newton, M. J.; Cheung, R. Tunable Graphene-Polymer Resonators for Audio Frequency Sensing Applications. *IEEE Sens. J.* **2019**, *19*, 465–473.

(19) Xu, J.; Wood, G. S.; Al-mashaal, A. K.; Mastropaolo, E.; Newton, M. J.; Cheung, R. Realization of Closed Cavity Resonator Formed by Graphene-PMMA Membrane for Sensing Audio Frequency. *IEEE Sens. J.* **2020**, *20*, 4618–4627.

(20) Bergqvist, J.; Gobet, J. Capacitive Microphone with a Surface Micromachined Backplate Using Electroplating Technology. *J. Microelectromech. Syst.* **1994**, *3*, 69–75.

(21) Li, P.; You, Z.; Cui, T. Graphene Cantilever Beams for Nano Switches. *Appl. Phys. Lett.* **2012**, *101*, 093111.

(22) Eichler, A.; Moser, J.; Chaste, J.; Zdrojek, M.; Wilson-Rae, I.; Bachtold, A. Nonlinear Damping in Mechanical Resonators Made from Carbon Nanotubes and Graphene. *Nat. Nanotechnol.* **2011**, *6*, 339–342.

(23) Chen, C.; Rosenblatt, S.; Bolotin, K. I.; Kalb, W.; Kim, P.; Kymissis, I.; Stormer, H. L.; Heinz, T. F.; Hone, J. Performance of Monolayer Graphene Nanomechanical Resonators with Electrical Readout. *Nat. Nanotechnol.* **2009**, *4*, 861–867.

(24) Singh, V.; Sengupta, S.; Solanki, H. S.; Dhall, R.; Allain, A.; Dhara, S.; Pant, P.; Deshmukh, M. M. Probing Thermal Expansion of Graphene and Modal Dispersion at Low-Temperature Using Graphene Nanoelectromechanical Systems Resonators. *Nanotechnology* **2010**, *21*, 165204.

(25) Al-mashaal, A. K.; Wood, G. S.; Torin, A.; Mastropaolo, E.; Newton, M. J.; Cheung, R. Dynamic Behavior of Ultra Large Graphene-based Membranes Using Electrothermal Transduction. *Appl. Phys. Lett.* **2017**, *111*, 243503.

(26) Chen, K.; Saltzman, E. J.; Schweizer, K. S. Segmental Dynamics in Polymers: from Cold Melts to Ageing and Stressed Glasses. *J. Phys.: Condens. Matter* **2009**, *21*, 503101.

(27) Ogata, K. *Modern Control Engineering*; Prentice Hall, 2010, pp 492–588.

■ NOTE ADDED AFTER ASAP PUBLICATION

This paper was published ASAP on July 31, 2021. A correction was made to the title and the corrected version was reposted on August 3, 2021.